Atmos. Chem. Phys., 19, 10469–10479, 2019
https://doi.org/10.5194/acp-19-10469-2019

Atmospheric Chemistry and Physics
Open Access
EGU

Enrichment of submicron sea-salt-containing particles in small cloud droplets based on single-particle mass spectrometry

Qinhao Lin[1], Yuxiang Yang[1,2], Yuzhen Fu[1,2], Guohua Zhang[1], Feng Jiang[1,2], Long Peng[1,2], Xiufeng Lian[1,2], Fengxian Liu[1,2,a], Xinhui Bi[1], Lei Li[3], Duohong Chen[4], Mei Li[3], Jie Ou[5], Mingjin Tang[1], Xinming Wang[1], Ping'an Peng[1], and Guoying Sheng[1]

[1]State Key Laboratory of Organic Geochemistry and Guangdong Key Laboratory of Environmental Resources Utilization and Protection, Guangzhou Institute of Geochemistry, Chinese Academy of Sciences, Guangzhou 510640, PR China
[2]University of Chinese Academy of Sciences, Beijing 100039, PR China
[3]Institute of Mass Spectrometer and Atmospheric Environment, Jinan University, Guangzhou 510632, PR China
[4]State Environmental Protection Key Laboratory of Regional Air Quality Monitoring, Guangdong Environmental Monitoring Center, Guangzhou 510308, PR China
[5]Shaoguan Environmental Monitoring Center, Shaoguan 512026, PR China
[a]currently at: College of Economics and Management, Taiyuan University of Technology, Taiyuan 030024, PR China

Correspondence: Xinhui Bi (bixh@gig.ac.cn)

Received: 12 February 2019 – Discussion started: 26 April 2019
Revised: 4 July 2019 – Accepted: 31 July 2019 – Published: 20 August 2019

Abstract. The effects of the chemical composition and size of sea-salt-containing particles on their cloud condensation nuclei (CCN) activity are incompletely understood. We used a ground-based counterflow virtual impactor (GCVI) coupled with a single-particle aerosol mass spectrometer (SPAMS) to characterize chemical composition of submicron (dry diameter of 0.2–1.0 µm) and supermicron (1.0–2.0 µm) sea-salt-containing cloud residues (dried cloud droplets) at Mount Nanling, southern China. Seven cut sizes (7.5–14 µm) of cloud droplets were set in the GCVI system. The highest number fraction of sea-salt-containing particles was observed at the cut size of 7.5 µm (26 %, by number), followed by 14 µm (17 %) and the other cut sizes (3 %–5 %). The submicron sea-salt-containing cloud residues contributed approximately 20 % (by number) at the cut size of 7.5 µm, which was significantly higher than the percentages at the cut sizes of 8–14 µm (below 2 %). This difference was likely involved in the change in the chemical composition. At the cut size of 7.5 µm, nitrate was internally mixed with over 90 % of the submicron sea-salt-containing cloud residues, which was higher than sulfate (20 %), ammonium (below 1 %), amines (6 %), hydrocarbon organic species (2 %), and organic acids (4 %). However, at the cut sizes of 8–14 µm, nitrate, sulfate, ammonium, amines, hydrocarbon organic species, and organic acids were internally mixed with > 90 %, > 80 %, 39 %–84 %, 71 %–86 %, 52 %–90 %, and 32 %–77 % of the submicron sea-salt-containing cloud residues. The proportion of sea-salt-containing particles in the supermicron cloud residues generally increased as a function of cut size, and their CCN activity was less influenced by chemical composition. This study provided a significant contribution towards a comprehensive understanding of sea-salt CCN activity.

1 Introduction

Atmospheric aerosol particles can directly influence the global radiative forces by scattering and absorbing solar radiation, and can indirectly influence them by serving as cloud condensation nuclei (CCN) (Boucher et al., 2013). The oceans represent one of the largest sources of natural aerosols, with an estimated global production rate of 2000–10 000 Tg per year (Gantt and Meskhidze, 2013). Modeling simulations showed that the indirect radiative forces of sea-salt particles were about twice those of the direct forces (Ma et al., 2008). The addition of the sea-salt particles over the remote ocean was estimated to enhance its CCN concentration

by up to 500 % (Pierce and Adams, 2006). The ability of sea-salt particles acting as CCN is dependent on their size and chemical composition at a specific supersaturation (Andreae and Rosenfeld, 2008). Therefore, it is important to evaluate the impact of chemical composition and particle size on the CCN behavior of sea-salt particles.

Numerous studies have revealed that fresh sea-salt particles consist of inorganic salts and biologically produced organic species rather than just sodium chloride (NaCl) (Prather et al., 2013; Quinn et al., 2015; Bertram et al., 2018). The size-resolved chemical composition of fresh sea-spray aerosols is dependent on complex factors including biological sources (e.g., phytoplankton and bacteria), physicochemical (e.g., sea-surface active organic species) properties, and wind speeds (Quinn et al., 2015). Previous studies have shown that an increasing fraction of fresh sea-salt particles is an internal mixture of inorganic salts (mainly including NaCl) and organic species as a result of the decreasing particle size (Prather et al., 2013; Bertram et al., 2018). However, the fraction of organics (i.e., aliphatic organic material) in small sea-spray aerosols exhibited some levels of variability in the similar simulation of ocean seawater conditions (Wang et al., 2015). Heterogeneous/multiphase reactions or atmospheric aging processes during transport can further lead to the size-dependent change in the chemical composition of sea-salt particles (Dall'Osto et al., 2004; Chi et al., 2015; Bondy et al., 2017). Bondy et al. (2017) found that sulfate was enriched in the submicron sea-salt particles, while nitrate dominated in the supermicron sea-salt particles (Bondy et al., 2017). However, Kirpes et al. (2018) observed that sulfate was also more prevalent than nitrate in supermicron sea-salt particles (Kirpes et al., 2018). Additionally, sea-salt particles could also react with various organic acids (e.g., oxalate, malonate, and succinate) during transport (Mochida et al., 2003; Laskin et al., 2012). Uncertainty in the formation of secondary species (e.g., sulfate, nitrate, or organic species) would complicate the size-dependent change in the chemical composition of sea-salt particles and thus the CCN activity.

Twohy et al. (1989) observed that small ammonium sulfate particles grew to small droplets and large sea-salt particles grew to large droplets. Previous observations also considered that the supermicron or giant sea-salt-containing particles readily became large cloud droplets, and their CCN behavior was less affected by chemical composition (Noone et al., 1988; Monger et al., 1989; Andreae and Rosenfeld, 2008; Tao et al., 2012). So far, studies on the submicron sea-salt-containing particles in cloud droplets have been scarce in the literature. Additionally, the existence of secondary species (e.g., sulfate, nitrate, or organic species) on the submicron sea-salt-containing particles might significantly impact their cloud activation (O'Dowd et al., 1999; Gibson et al., 2006; Nguyen et al., 2017).

In this study, a ground-based counterflow virtual impactor (GCVI) combined with an online single-particle aerosol mass spectrometer (SPAMS) was used to characterize the chemical composition of sea-salt-containing cloud residues at Mount Nanling, southern China. This was performed in the downwind direction from the South China Sea during the study period of May–June 2017. The main goal of this work was to identify the discrepancies in the relative contributions of sea-salt-containing particles as a function of the cloud droplet cut size (>7.5, >8.0, >8.5, >9.0, >10.0, >11.0, and >14.0 µm were set in the GCVI system). To elucidate the cloud activity of submicron (dry diameter of 0.2–1.0 µm) sea-salt-containing particles, the chemical composition of submicron sea-salt-containing particles within various cloud droplet cut sizes was also addressed.

2 Experimental section

2.1 Observation site

The sampling site, which is a National Air Background Monitoring Station, is situated at Mount Nanling, southern China (112°53′56″ E, 24°41′56″ N at 1690 m above sea level). This station is surrounded by a national park forest (273 km^2) minimally affected by local anthropogenic activities. The sampling site is located 50–100 km northeast or north of the Pearl River delta (PRD) urban agglomeration and 350 km north of the South China Sea (Fig. S1 in the Supplement). The sampling site is affected by the East Asian summer monsoon system (Ding and Chan, 2005). Generally, air masses would spend some time traveling across the South China Sea and then travel over the PRD region before reaching the sampling site during the summer period. The SO_2, NO_x, NH_3, and volatile organic compound emissions in the PRD region are approximately 711, 891, 195, and 1180 kiloton per year, respectively (Zheng et al., 2009, 2012). Hence, the sea-salt-containing particles that originate from the South China Sea could interact with anthropogenic gaseous pollutants during their movement across the PRD region.

2.2 Instrumentation

The measurements took place from 18 May to 11 June 2017. The real-time air quality and meteorological parameters were continuously monitored. A GCVI inlet system (GCVI Model 1205, Brechtel Manufacturing Inc.) was used to sample the cloud droplets with various cut sizes. The cloud droplet cut sizes and duration time set in the GCVI system are presented in Table S1 in the Supplement. The minimum sampling time for each cut size was 12 h. The cut size was adjusted by modifying the air velocity in the wind tunnel of the GCVI inlet system (Shingler et al., 2012). It should be noted here that the transmission efficiency increased as the cut size increased (Shingler et al., 2012). The sampled cloud droplets passed through an evaporation chamber to remove the water and the dry residue particles remained. The enrichment factor of the particles that were collected by the GCVI inlet was estimated to range from 6.6 in 7.5 µm to 2.0

in 14.0 µm based on theoretical calculations (Shingler et al., 2012). Pekour and Cziczo (2011) observed that the breakthrough of large particles tended to increase at the lower size cut. In this study, the number concentration of ambient particles in the GCVI downstream inlet was below 1 cm^3 at the lowest cut sizes during cloud-free periods, and hence the large particle breakthrough at the lowest cut size seemed to be quite low. The cloud residues were subsequently characterized using an online SPAMS (Hexin Analytical Instrument Co., Ltd., Guangzhou, China). In order to reliably identify the presence of clouds, an upper-limit visibility of 3 km and a lower-limit relative humidity (RH) of 95 % were set in the GCVI software (Lin et al., 2017). During precipitation periods, the GCVI automatically shut down to protect against interference from raindrops.

The SPAMS conducts the real-time characterization of the chemical composition of aerosol particles using vacuum aerodynamic diameters (d_{va}) between 0.2 and 2.0 µm. The detailed operations of the SPAMS have been described elsewhere (Li et al., 2011). Briefly, aerosol particles are introduced into the SPAMS through a nozzle inlet. The particle velocity is derived from the measurement of two continuous diode Nd : YAG laser beams (532 nm) and is then converted to the particle size (d_{va}). The particles are subsequently desorbed and ionized by a pulsed laser (266 nm). The positive and negative mass spectra generated are recorded with the corresponding particle size. The laser pulse energy was regulated at 0.5–0.6 mJ during the whole sampling period. Polystyrene latex spheres (Nanosphere Size Standards, Duke Scientific Corp., Palo Alto) of 0.2–2.0 µm in diameter were used to calibrate the sizes of the detected particles. It should be noted that the particles detected by the SPAMS are mostly in the size range of d_{va} 0.2–2.0 µm (Li et al., 2011).

2.3 Screening of sea-salt-containing particles

According to prior laboratory and field studies, sea-salt-containing particles generally exhibit a set of sodium-related peaks at m/z 23 $[Na]^+$, 46 $[Na_2]^+$, 62 $[Na_2O]^+$, 63 $[Na_2OH]^+$, 81 $[Na_2^{35}Cl]^+$, and 83 $[Na_2^{37}Cl]^+$ (Dall'Osto et al., 2004; Herich et al., 2009; Prather et al., 2013). Thus, the sea-salt-containing particles in this study were identified by the simultaneous existence of peaks at m/z 23, 46, 62, 63, 81, and 83. Because biologically produced organic species (e.g., m/z −26 $[CN]^-$, −42 $[CNO]^-$, or 59 $[NC_3H_9]^+$) were internally mixed with sodium-related peaks (Prather et al., 2013; Sultana et al., 2017), these primary organic species were not intended to define sea-salt-containing particles. Additionally, these organic species might also be produced from secondary aerosol processes (Dall'Osto et al., 2009; Zhang et al., 2012). Therefore, biologically produced organic species that externally mixed with sea-salt particles were not considered in the current study. One may expect that chlorine ion peaks at m/z −35 $[^{35}Cl]^-$ or −37 $[^{37}Cl]^-$ in the negative mass spectrum should be considered. Sea-salt-containing particles in the atmosphere might not contain chloride due to the complete displacement of chloride by sulfate, nitrate, or organic acids during transport (Laskin et al., 2012; Ueda et al., 2014; Arndt et al., 2017). Bondy et al. (2017) also suggested that the identification of sea-salt-containing particles without using chloride might give more detailed results on the atmospheric aging processes during transport (Bondy et al., 2017). Thus, a total of 30 275 sea-salt-containing cloud residues including 8317 submicron and 21 958 supermicron particles were obtained in this study.

3 Results and discussion

3.1 General characteristics

Figure 1 displays the hourly averaged data of the meteorological and air quality parameters during the whole sampling period. The wind direction prevailed southwesterly or southerly during the cloud events and most corresponding air masses originated from the South China Sea (Fig. S2), which had abundant moist airflows that were probably responsible for the formation of the cloud events. The maximum concentrations of $PM_{2.5}$, SO_2, and NO_x were 76 µg m^{-3}, 2.8, and 12 ppb, respectively, during the cloud-free periods. When the cloud events occurred, the levels of $PM_{2.5}$, SO_2, and NO_x clearly decreased, which was indicative of cloud scavenging. The ambient temperature was above 10 °C during the whole study period, which allows the formation of liquid cloud droplets.

The average mass spectrum of the sea-salt-containing cloud residues during the sampling period is shown in Fig. 2. The highest peak at m/z 23 and some small ion peaks at m/z 24 $[Mg]^+$, 39 $[K]^+$, 40 $[Ca]^+$, and 56 $[CaO]^+$ or $[Fe]^+$ were observed in the positive mass spectra. This result was in agreement with the previous findings from laboratory and field studies (Guazzotti et al., 2001; Dall'Osto et al., 2004; Gaston et al., 2011; Prather et al., 2013). The significant ion peaks at m/z −46 $[NO_2]^-$ or −62 $[NO_3]^-$ and −97 $[HSO_4]^-$ in the negative mass spectrum represented nitrate and sulfate markers, thus suggesting aged sea-salt-containing cloud residues. The presence of organic nitrogen peaks at m/z −26 $[CN]^-$ or −42 $[CNO]^-$ in the negative mass spectrum may be from biologically produced sources or the subsequent accumulation of secondary organic aerosols (Herich et al., 2009; Prather et al., 2013). The small peak areas of other organic species including hydrocarbon organic species (i.e., m/z 15 $[CH_3]^+$, m/z 27 $[C_2H_3]^+$ or m/z 43 $[C_2H_3O]^+$), amines (m/z 59 $[C_3H_9N]^+$ or 86 $[C_5H_{12}N]^+$), or organic acids (m/z −89 oxalate, −103 malonate, or −117 succinate) can also be detected in the sea-salt-containing cloud residues (Fig. S3).

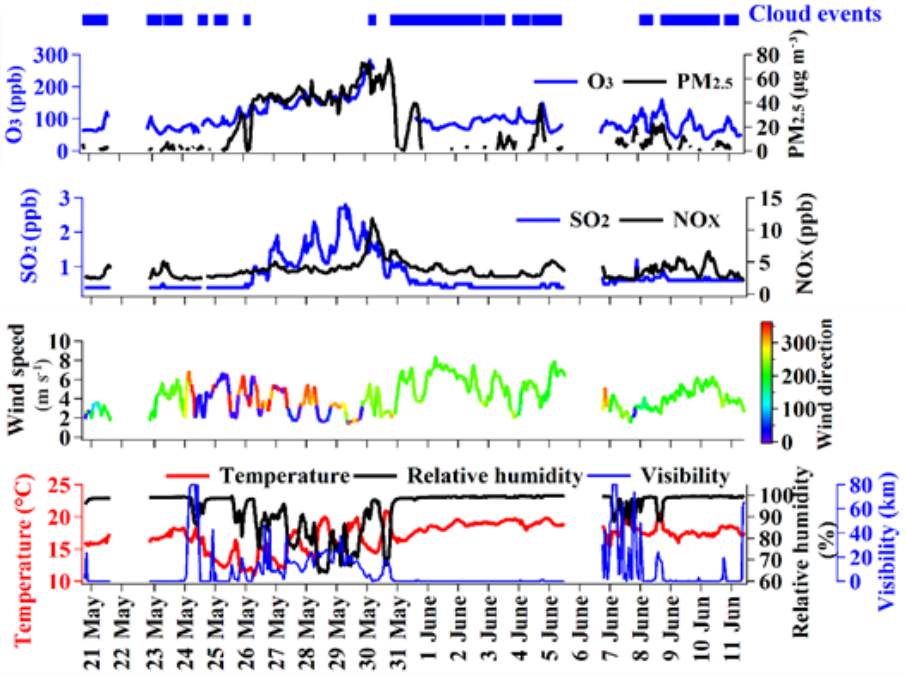

Figure 1. The hourly averaged data of meteorological and air quality parameters.

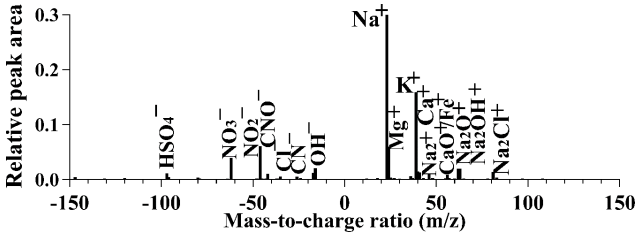

Figure 2. The averaged mass spectrum of the sea-salt-containing cloud residues.

3.2 Number fraction and chemical composition of sea-salt-containing cloud residues

The number fraction (NF) of sea-salt-containing particles in the total cloud residues was dependent on the cut sizes. The highest NF was observed at the cut size of 7.5 µm (26 %, by number), followed by 14 µm (17 %) and the other cut sizes (3 %–5 %) (Fig. 3a). These values were higher than the NF (2 %, by number) of sea-salt-containing particles in the detected ambient aerosol particles during cloud-free periods. Sea-salt-containing particles contributed approximately 1 % (by number) of cloud residues at the cut size of 5.0 µm over Mount Schmücke in central Germany, despite air masses that frequently originated over the Atlantic Ocean (Roth et al., 2016). The proportion reached 5 %–10 % (by number) at the cut size of 11 µm at the North Slope of Alaska (Zelenyuk et al., 2010). Additionally, the cloud water measurement showed that sea-salt-containing particles might accumulate in large cloud droplets (Monger et al., 1989). In contrast to these findings, the maximum NF of sea-salt-containing cloud residues was found at the minimum GCVI cut size in this study. Twohy and Anderson (2008) observed an increased NF of sea-salt-like cloud residues from coastal areas at the cut size of 20 µm to clean remote oceans at the cut size of 8 µm (Twohy and Anderson, 2008). However, it cannot interpret the enhancement of sea-salt-containing cloud residues at the cut size of 7.5 µm in this study because of the comparable air quality and meteorological environments at all the cut sizes.

There was a significant difference in the chemical composition of the sea-salt-containing cloud residues between the cut sizes of 7.5 µm and 8–14 µm, as shown in Fig. 4. Nitrate was internally mixed with above 90 % of the sea-salt-containing cloud residues at all the cut sizes. However, notably decreased sulfate (32 % versus 87 %–93 %, by number), ammonium (below 1 % versus 21 %–32 %), organic nitrogen (70 % versus 87 %–96 %), amines (6 % versus 30 %–64 %), hydrocarbon organics (2 % versus 22 %–70 %), and organic acids (7 % versus 42 %–76 %) were found internally mixed with the sea-salt-containing cloud residues at the cut size of 7.5 µm compared to 8–14 µm. Roth et al. (2016) found that both sulfate and nitrate were internally mixed with the sea-salt-containing cloud residues (Roth et al., 2016). Another study by Zelenyuk et al. (2010) observed that the sea-salt-containing cloud residues were composed of four particle types, including fresh NaCl, NaCl internally mixed with nitrate, sulfate, and organics. In this study, abundant nitrate was found to internally mix with the sea-salt-containing

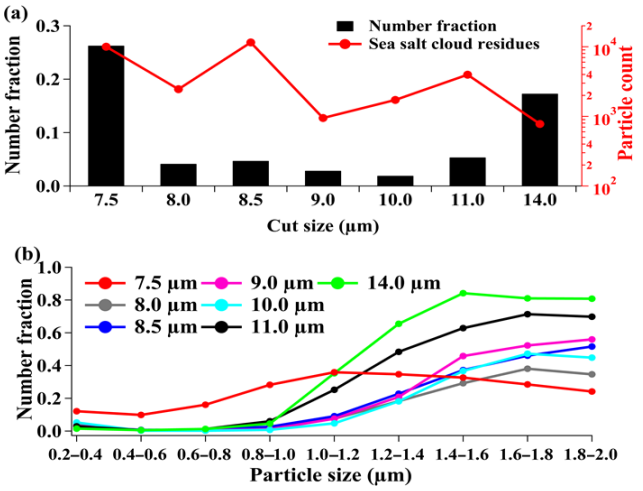

Figure 3. Number fraction or counts of sea-salt-containing cloud residues as a function of the cut size **(a)** and the relative contribution of sea-salt-containing cloud residues to the total cloud residues in the given size range **(b)**.

cloud residues at all the cut sizes, while sulfate, ammonium, and organic species showed more diversity between the cut sizes of 7.5 and 8–14 µm. These differences in the chemical mixtures of sea-salt-containing cloud residues dependent on the location suggest that sea-salt-containing particles would experience various aging process in the atmosphere and subsequently participate in the formation of cloud droplets. More importantly, together with the enrichment of sea-salt-containing cloud residues at the minimum cut size of 7.5 µm observed here, this might indicate that the distribution of sea-salt-containing cloud residues that were dependent on cloud droplet size is likely influenced by changes in the chemical mixtures of sea-salt-containing nuclei. It should be noted here that, relative to small cloud droplets, larger cloud droplets might undergo longer-duration cloud (Nakajima et al., 2010), thus increasing the in-cloud formation of secondary species such as sulfate, ammonium, or oxalate. The extreme high fraction of nitrate in the sea-salt-containing cloud residues at all the cut sizes was more likely due to the aging processes during atmospheric transport, rather than the in-cloud formation.

It is well-known that the chloride depletion in sea-salt-containing particles is mainly due to the formation of secondary species, such as sulfate, nitrate, or organic acids (Laskin et al., 2012; Bondy et al., 2017). The chloride depletion might lower the hygroscopic and CCN properties of sea-salt-containing particles (i.e., NaCl) (O'Dowd et al., 1999; Gupta et al., 2015). In this study, chloride was internally mixed with above 80 % (by number) of the sea-salt-containing cloud residues at the cut sizes of 8–14 µm, which was clearly higher than 51 % at the cut size of 7.5 µm. That is, chloride depletion was weakened in the sea-salt-containing cloud residues at the cut sizes of 8–14 µm, despite abundant sulfate and organic acids, as mentioned above. Based on a laboratory study, Ault et al. (2014) found that organic nitrogen can inhibit the heterogeneous reaction of sea-salt-containing particles with HNO_3 (Ault et al., 2014). They used a peak area ratio of chloride to (chloride + nitrate) to estimate the extent of the chloride depletion (Ault et al., 2014). Because the heterogeneous reaction with H_2SO_4, HNO_3, or organic acids and sea-salt-containing particles is also present in the atmosphere (Laskin et al., 2012; Chi et al., 2015), a modified peak area ratio (chloride/(chloride + nitrate + sulfate + organic acids)) was applied in the present study. This ratio was found to increase as a function of the increase in the peak area of organic nitrogen, as shown in Fig. 5, thereby reflecting the effect of organic nitrogen on the depletion of chloride in sea-salt-containing particles in the atmosphere. At the cut sizes of 8–14 µm, abundant organic nitrogen in the sea-salt-containing cloud residues likely lowered the chloride depletion. The ratio was not found to be related to the hydrocarbon organic species. The sensitivity of chloride displacement to the presence of organic species was complex (Ault et al., 2014; Bertram et al., 2018), and further studies must be conducted to identify whether diverse organic species affect the heterogeneous reactivity of individual sea-salt-containing particles.

3.3 Submicron sea-salt-containing cloud residues

The modeling calculation showed that submicron sea-salt-containing particles may have a dominant contribution to aerosol–cloud interactions when evaluating the indirect impacts of sea-salt aerosols, despite the uncertainty in the sizes and concentrations of sea-salt aerosols (Gong, 2003). Few field studies have focused on the submicron sea-salt-containing particles within cloud droplets. In this work, approximately 25 % (by number) of the sea-salt-containing cloud residues was found to be at the submicron size. It should be noted that the size distribution of the sea-salt-containing cloud residues that were detected by the SPAMS cannot represent the real atmosphere because the highest detection efficiency for the SPAMS was in the size range of 500–800 nm (Li et al., 2011). The relative contribution of sea-salt-containing particles to the cloud residues in the given size range is presented to eliminate the detection efficiency of single-particle mass spectrometry (Roth et al., 2016), as shown in Fig. 3b. At the cut size of 7.5 µm, 20 % (by number) of the submicron cloud residues was composed of sea-salt-containing particles. This value was prominently higher than that at the cut sizes of 8–14 µm (below 2 %, by number) or that during cloud-free periods (1 %) (Fig. S4). The difference at least reflects that the submicron sea-salt-containing particles could be enriched in the small cloud droplets.

The diverse chemical composition of the submicron sea-salt-containing cloud residues was found between the cut sizes of 7.5 and 8–14 µm. At the cut size of 7.5 µm, nitrate was internally mixed with 90 % (by number) of the sub-

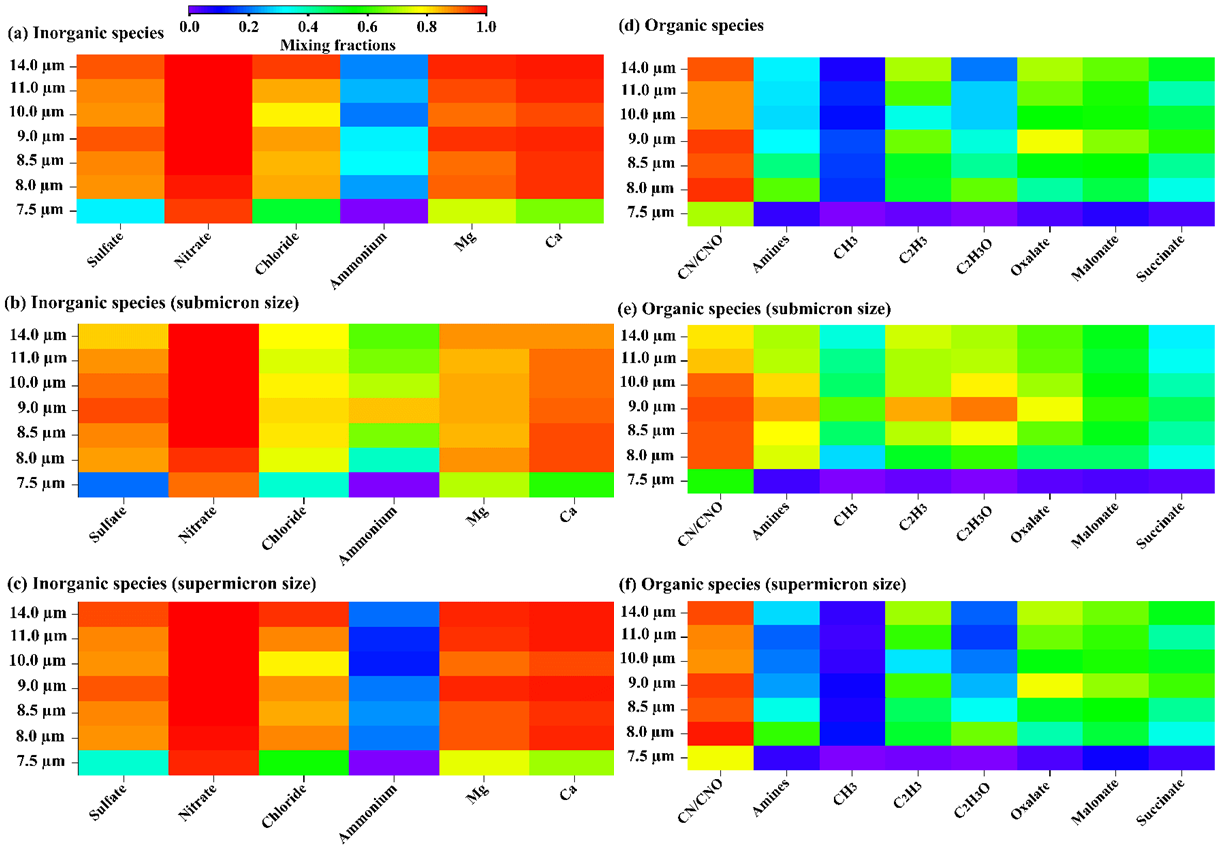

Figure 4. Mixed fractions of inorganic and organic species in the sea-salt-containing cloud residues. The mixing fraction is defined as the number of particles of a given compound divided by the total number of particles. The inorganic species include sulfate (m/z −97), nitrate (m/z −46 or −62), chloride (m/z −35 or −37), ammonium (m/z 18), magnesium (m/z 24), and calcium (m/z 40). The organic species include organic nitrogen (m/z −26 or −42), amines (m/z 59 or 86), CH_3 (m/z 15), C_2H_3 (m/z 27), C_2H_3O (m/z 43), oxalate (m/z −89), malonate (m/z −103), and succinate (m/z −117).

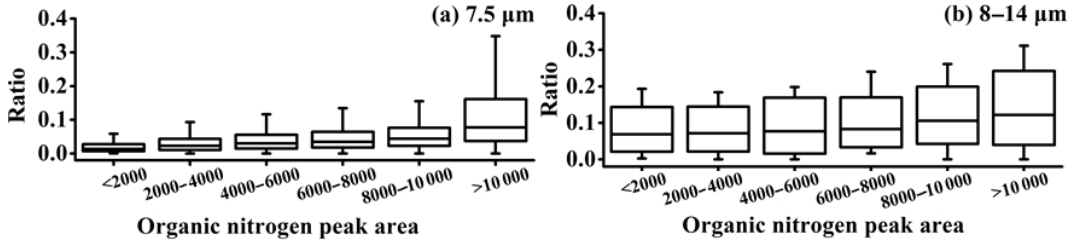

Figure 5. Ratio as a function of the organic nitrogen (m/z −26 or −42) peak area. The ratio refers to the chloride (m/z −35 or −37) peak area divided by the sum of the sulfate (m/z −97), nitrate (m/z −46 or −62), organic acids (m/z −89, −103, or −117), and chloride peak areas, as explained in the text.

micron sea-salt-containing cloud residues, which was much higher than the fractions of sulfate (20 %) and ammonium (below 1 %) (Fig. 4). It implies that the secondary inorganic species in the submicron sea-salt-containing cloud residues at the cut size of 7.5 µm was dominated by nitrate, mostly from the partitioning and heterogeneous/aqueous chemistry of HNO_3 and other precursors (e.g., N_2O_5) in the atmosphere (Chang et al., 2011; Schneider et al., 2017). However, prominently higher fractions of sulfate (86 %–94 %, by number) and ammonium (38 %–83 %) were found to internally mix with the submicron sea-salt-containing cloud residues at the cut sizes of 8–14 µm, thus reflecting more chemically aged or longer cloud processes. This was also supported by the increase in the relative peak areas of these secondary species in the submicron sea-salt-containing cloud residues at the cut sizes of 8–14 µm compared to 7.5 µm (Fig. S5). The enrich-

ment of sulfate in the submicron sea-salt-containing particles has also been reported extensively in the literature (Jourdain et al., 2008; Kelly et al., 2010; Bondy et al., 2017), which is largely a result of the preferential formation of sulfate in submicron particle sizes with great surface area-to-volume ratios (Song and Carmichael, 1999). Initially, fresh sea-salt-containing particles generally appear to be alkaline due to carbonate, and they subsequently experience the reactive uptake of SO_2, H_2SO_4, or HNO_3 during transport (Sievering et al., 1999; Alexander et al., 2005). The lack of ammonium suggests that the accumulated secondary acids during transport insufficiently acidize the submicron sea-salt-containing cloud residues at the cut size of 7.5 µm, which, in turn, causes the uptake of gaseous NH_3 to fail. In contrast, the accumulated ammonium in the submicron sea-salt-containing cloud residues at the cut sizes of 8–14 µm (Fig. 4) indicate that the alkaline sea-salt-containing cloud residues have been eventually consumed by secondary acids and thus uptake gaseous NH_3 to neutralize these acidic species (Song and Carmichael, 1999). Furthermore, a higher number fraction of amines was found to internally mix with the submicron sea-salt-containing cloud residues at the cut sizes of 8–14 µm compared to 7.5 µm (71 %–87 % versus 6 %, by number). Despite the biologically produced amines being internally mixed with fresh sea-salt-containing particles (Sultana et al., 2017), a similar feature of ammonium and amines in the submicron sea-salt-containing cloud residues observed here implies that the presence of amines mainly comes from the partitioning of the gas into the aqueous phase, particularly during cloud processing (Roth et al., 2016; Lin et al., 2017).

A laboratory study showed that biologically produced organic nitrogen that internally mixed with fresh sea-salt-containing particles was found to increase in the submicron size range (Prather et al., 2013). This likely led to the enrichment of organic nitrogen (58 %, by number) relative to hydrocarbon organic species (2 %) or organic acids (4 %) in the submicron sea-salt-containing cloud residues at the cut size of 7.5 µm (Fig. 4). Meanwhile, at the cut sizes of 8–14 µm, higher fractions of organic nitrogen (80 %–94 %, by number), hydrocarbon organic species (52 %–90 %), and organic acids (32 %–77 %) were observed (Fig. 4), indicative of the more chemically aged processes, as mentioned above. Note that magnesium and calcium internally mixed with above 85 % (by number) and above 88 % of the submicron sea-salt-containing cloud residues at the cut sizes of 8–14 µm might increase the presence of organic nitrogen due to the probable complexation with organic species and these cations (Bertram et al., 2018). Hydrocarbon organic particle types coupled with the peak area $Mg \gg Na$ can be produced from biological sources in seawater, but they are externally mixed with fresh submicron sea-salt-containing particles (Sultana et al., 2017). Thus, the abundant hydrocarbon organics observed here might originate from accumulation during transport. The uptake of gaseous organic acids or the organic acids that formed through heterogeneous reactions were responsible for the increased organic acids presented herein (Mochida et al., 2003; Sullivan and Prather, 2007). We cannot preclude that the decreased organic species of the submicron sea-salt-containing particles at the cut size of 7.5 µm might also be due to having shorter-duration cloud relative to other cut sizes. Further study needs to compare the contribution of aging degree during transport and duration time of cloud process to the secondary species.

Petters and Kreidenweis (2007) described the CCN activity of multicomponent aerosol particles using a single parameter (κ) as follows: $\kappa = \varepsilon_{org} \cdot \kappa_{org} + \varepsilon_{inorg} \cdot \kappa_{inorg}$, where ε_{org} and ε_{inorg} represent the bulk volume fractions of organic and inorganic species, respectively, and κ_{org} (generally below 0.5 for organic species) and κ_{inorg} (1.28 for NaCl, 0.88 for $NaNO_3$, 0.80 for Na_2SO_4, 0.67 for NH_4NO_3, and 0.61 for $(NH_4)_2SO_4$) refer to the CCN-derived hygroscopicity parameters of the organic and inorganic species, respectively. Relative to the cut sizes of 8–14 µm, the reduction of organic species in the submicron sea-salt-containing cloud residues at the cut size of 7.5 µm is likely to increase κ and hence CCN property. Additionally, the submicron sea-salt particles contained higher proportions of organic nitrogen (73 %–94 % versus 58 %, by number), hydrocarbon organic species (51 %–81 % versus 2 %), and organic acids (35 %–72 % versus 4 %) in the ambient aerosol particles than in the cloud residues at the cut size of 7.5 µm. This further indicates that the enhancement of organic species in the submicron particles likely reduced CCN activity of sea-salt particles.

3.4 Supermicron sea-salt-containing cloud residues

The supermicron (dry diameter of 1.0–2.0 µm) sea-salt-containing particles contributed more to cloud residues with the increasing cut sizes (Fig. 3b). For instance, up to 70 % of the supermicron cloud residues were found to consist of sea-salt-containing particles at the maximum cut size of 14 µm. The enrichment of the large supermicron or giant sea-salt-containing particles in large cloud droplets has also been reported in previous studies (Noone et al., 1988; Twohy et al., 1989; Tao et al., 2012). Nitrate was internally mixed with above 90 % (by number) of the supermicron sea-salt-containing cloud residues at all the cut sizes (Fig. 4). The proportions of sulfate, ammonium, and organic species in supermicron sea-salt-containing cloud residues at the cut size of 7.5 µm were lower than those at the cut sizes of 8–14 µm (Fig. 4), which was similar to the submicron particles. However, the increased organic species in the supermicron sea-salt-containing cloud residues at the cut sizes of 8–14 µm were not expected to reduce their CCN behavior. It was likely that their CCN activity was less affected by the change in the chemical composition. For coarse or giant nuclei (dry particle size > 1 µm), their CCN abilities were dependent on their size rather than their chemical composition (Andreae and Rosenfeld, 2008; Tao et al., 2012). Hud-

son and Rogers (1986) also found that large nuclei increased in large cloud droplets due to lower critical supersaturation of larger nuclei compared to smaller nuclei (Hudson and Rogers, 1986).

4 Atmospheric implications and conclusion

This work focused on the size-resolved chemical composition of sea-salt-containing cloud residues as a function of the cloud droplet cut size. Nitrate internally mixed with above 95 % (by number) of the sea-salt-containing cloud residues at all the cut sizes emphasized that the sea-salt-containing nuclei had undergone chemical evolution during transport. For simplicity, modeling simulations assumed that the externally mixed NaCl and secondary species (e.g., sulfate) mode or pure NaCl instead of sea-salt aerosols was used to predict the size-dependent cloud droplet chemistry or the residence time of sea-salt aerosols in the atmosphere (Twohy et al., 1989; Gong et al., 2002; Ma et al., 2008). The change in chemical composition of the submicron sea-salt-containing particles might have an impact on their CCN activity. Our result showed that the reduction of organic species in the submicron sea-salt-containing cloud residues at the cut size of 7.5 µm is likely to increase CCN activity, leading to the enrichment of the submicron sea-salt-containing particles. The resulting effect might prolong the residence time of submicron sea-salt-containing aerosols in the atmosphere. This differed from the supermicron sea-salt-containing particles, which readily become large cloud droplets, consistent with the previous measurements (Noone et al., 1988; Yuan et al., 2008). More work is needed to evaluate the contribution of atmospheric aged processes to the change in the chemical composition that is associated with the CCN activity of sea-salt-containing particles, particularly in the submicron size range.

Data availability. All the data can be obtained by contacting the corresponding author Xinhui Bi (bixh@gig.ac.cn).

Supplement. The supplement related to this article is available online at: https://doi.org/10.5194/acp-19-10469-2019-supplement.

Author contributions. XB, GZ, and QL planned and designed the experimental setup. YY, YF, LP, FJ, XL, FL, and JO performed the atmospheric measurement and collected the data. QL and XB analyzed the data and wrote the manuscript. LL, DC, ML, MT, XW, PAP, and GS contributed comments.

Competing interests. The authors declare that they have no conflict of interest.

Acknowledgements. This work was supported by the National Key Research and Development Program of China (2017YFC0210104), the National Natural Science Foundation of China (nos. 41877307, 41775124, and 41805103), the Foundation for Leading Talents of the Guangdong Province Government, and the State Key Laboratory of Organic Geochemistry (SKLOG2016-A05). The authors also acknowledge the NOAA Air Resources Laboratory for the provision of the HYSPLIT transport and dispersion model and READY website (https://www.ready.noaa.gov/HYSPLIT.php, last access: 16 August 2019) used in this publication. This is contribution no. IS-2733 from GIGCAS.

Financial support. This research has been supported by the National Key Research and Development Program of China (grant no. 2017YFC0210104), the National Natural Science Foundation of China (grant nos. 41877307, 41775124, and 41805103), and the State Key Laboratory of Organic Geochemistry (grant no. SKLOG2016-A05).

Review statement. This paper was edited by Markus Petters and reviewed by two anonymous referees.

References

Alexander, B., Park, R. J., Jacob, D. J., Li, Q. B., Yantosca, R. M., Savarino, J., Lee, C. C. W., and Thiemens, M. H.: Sulfate formation in sea-salt aerosols: Constraints from oxygen isotopes, J. Geophys. Res.-Atmos., 110, D10307, https://doi.org/10.1029/2004jd005659, 2005.

Andreae, M. O. and Rosenfeld, D.: Aerosol-cloud-precipitation interactions. Part 1, The nature and sources of cloud-active aerosols, Earth-Sci. Rev., 89, 13–41, https://doi.org/10.1016/j.earscirev.2008.03.001, 2008.

Arndt, J., Sciare, J., Mallet, M., Roberts, G. C., Marchand, N., Sartelet, K., Sellegri, K., Dulac, F., Healy, R. M., and Wenger, J. C.: Sources and mixing state of summertime background aerosol in the north-western Mediterranean basin, Atmos. Chem. Phys., 17, 6975–7001, https://doi.org/10.5194/acp-17-6975-2017, 2017.

Ault, A. P., Guasco, T. L., Baltrusaitis, J., Ryder, O. S., Trueblood, J. V., Collins, D. B., Ruppel, M. J., Cuadra-Rodriguez, L. A., Prather, K. A., and Grassian, V. H.: Heterogeneous reactivity of nitric acid with nascent sea spray aerosol: Large differences observed between and within individual particles, J. Phys. Chem. Lett., 5, 2493–2500, https://doi.org/10.1021/jz5008802, 2014.

Bertram, T. H., Cochran, R. E., Grassian, V. H., and Stone, E. A.: Sea spray aerosol chemical composition: Elemental and molecular mimics for laboratory studies of heterogeneous and multiphase reactions, Chem. Soc. Rev., 47, 2374–2400, https://doi.org/10.1039/C7CS00008A, 2018.

Bondy, A. L., Wang, B., Laskin, A., Craig, R. L., Nhliziyo, M. V., Bertman, S. B., Pratt, K. A., Shepson, P. B., and Ault, A. P.: Inland sea spray aerosol transport and incomplete chloride depletion: Varying degrees of reactive processing observed during SOAS, Environ. Sci. Technol., 51, 9533–9542, https://doi.org/10.1021/acs.est.7b02085, 2017.

Boucher, O., Randall, D., Artaxo, P., Bretherton, C., Feingold, G., Forster, P., Kerminen, V., Kondo, Y., Liao, H., Lohmann, U., Rasch, P., Satheesh, S., Sherwood, S., Stevens, B., and Zhang, X.: Clouds and Aerosols, in: Climate Change 2013: The Physical Science Basis, Contribution of Working Group I to the Fifth Assessment Report of the Intergovernmental Panel on Climate Change, edited by: Stocker, T. F., Qin, D., Plattner, G. K., Tignor, M., Allen, S. K., Boschung, J., Nauels, A., Xia, Y., Bex, V., and Midgley, P. M., Cambridge University Press, Cambridge, UK and New York, NY, USA, 571–657, 2013.

Chang, W. L., Bhave, P. V., Brown, S. S., Riemer, N., Stutz, J., and Dabdub, D.: Heterogeneous atmospheric chemistry, ambient measurements, and model calculations of N_2O_5: A review, Aerosol Sci. Tech., 45, 665–695, https://doi.org/10.1080/02786826.2010.551672, 2011.

Chi, J. W., Li, W. J., Zhang, D. Z., Zhang, J. C., Lin, Y. T., Shen, X. J., Sun, J. Y., Chen, J. M., Zhang, X. Y., Zhang, Y. M., and Wang, W. X.: Sea salt aerosols as a reactive surface for inorganic and organic acidic gases in the Arctic troposphere, Atmos. Chem. Phys., 15, 11341–11353, https://doi.org/10.5194/acp-15-11341-2015, 2015.

Dall'Osto, M., Beddows, D. C. S., Kinnersley, R. P., Harrison, R. M., Donovan, R. J., and Heal, M. R.: Characterization of individual airborne particles by using aerosol time-of-flight mass spectrometry at Mace Head, Ireland, J. Geophys. Res.-Atmos., 109, D21302, https://doi.org/10.1029/2004jd004747, 2004.

Dall'Osto, M., Harrison, R. M., Coe, H., and Williams, P.: Real-time secondary aerosol formation during a fog event in London, Atmos. Chem. Phys., 9, 2459–2469, https://doi.org/10.5194/acp-9-2459-2009, 2009.

Ding, Y. and Chan, J. C. L.: The East Asian summer monsoon: An overview, Meteorol. Atmos. Phys., 89, 117–142, https://doi.org/10.1007/s00703-005-0125-z, 2005.

Gantt, B. and Meskhidze, N.: The physical and chemical characteristics of marine primary organic aerosol: a review, Atmos. Chem. Phys., 13, 3979–3996, https://doi.org/10.5194/acp-13-3979-2013, 2013.

Gaston, C. J., Furutani, H., Guazzotti, S. A., Coffee, K. R., Bates, T. S., Quinn, P. K., Aluwihare, L. I., Mitchell, B. G., and Prather, K. A.: Unique ocean-derived particles serve as a proxy for changes in ocean chemistry, J. Geophys. Res.-Atmos., 116, D18310, https://doi.org/10.1029/2010JD015289, 2011.

Gibson, E. R., Hudson, P. K., and Grassian, V. H.: Physicochemical properties of nitrate aerosols: Implications for the atmosphere, J. Phys. Chem. A, 110, 11785–11799, https://doi.org/10.1021/jp063821k, 2006.

Gong, S. L.: A parameterization of sea-salt aerosol source function for sub- and super-micron particles, Global Biogeochem. Cy., 17, 1097, https://doi.org/10.1029/2003gb002079, 2003.

Gong, S. L., Barrie, L. A., and Lazare, M.: Canadian Aerosol Module (CAM): A size-segregated simulation of atmospheric aerosol processes for climate and air quality models 2, Global sea-salt aerosol and its budgets, J. Geophys. Res.-Atmos., 107, 4779, https://doi.org/10.1029/2001jd002004, 2002.

Guazzotti, S. A., Coffee, K. R., and Prather, K. A.: Continuous measurements of size-resolved particle chemistry during INDOEX-intensive field phase 99, J. Geophys. Res.-Atmos., 106, 28607–28627, https://doi.org/10.1029/2001jd900099, 2001.

Gupta, D., Kim, H., Park, G., Li, X., Eom, H.-J., and Ro, C.-U.: Hygroscopic properties of NaCl and $NaNO_3$ mixture particles as reacted inorganic sea-salt aerosol surrogates, Atmos. Chem. Phys., 15, 3379–3393, https://doi.org/10.5194/acp-15-3379-2015, 2015.

Herich, H., Kammermann, L., Friedman, B., Gross, D. S., Weingartner, E., Lohmann, U., Spichtinger, P., Gysel, M., Baltensperger, U., and Cziczo, D. J.: Subarctic atmospheric aerosol composition: 2. Hygroscopic growth properties, J. Geophys. Res.-Atmos., 114, D13204, https://doi.org/10.1029/2008jd011574, 2009.

Hudson, J. G. and Rogers, C. F.: Relationship between critical supersaturation and cloud droplets size-implications for cloud mixing processes, J. Atmos. Sci., 43, 2341–2359, https://doi.org/10.1175/1520-0469(1986)043<2341:Rbcsac>2.0.Co;2, 1986.

Jourdain, B., Preunkert, S., Cerri, O., Castebrunet, H., Udisti, R., and Legrand, M.: Year-round record of size-segregated aerosol composition in central Antarctica (Concordia station): Implications for the degree of fractionation of sea-salt particles, J. Geophys. Res.-Atmos., 113, D14308, https://doi.org/10.1029/2007jd009584, 2008.

Kelly, J. T., Bhave, P. V., Nolte, C. G., Shankar, U., and Foley, K. M.: Simulating emission and chemical evolution of coarse sea-salt particles in the Community Multiscale Air Quality (CMAQ) model, Geosci. Model Dev., 3, 257–273, https://doi.org/10.5194/gmd-3-257-2010, 2010.

Kirpes, R. M., Bondy, A. L., Bonanno, D., Moffet, R. C., Wang, B., Laskin, A., Ault, A. P., and Pratt, K. A.: Secondary sulfate is internally mixed with sea spray aerosol and organic aerosol in the winter Arctic, Atmos. Chem. Phys., 18, 3937–3949, https://doi.org/10.5194/acp-18-3937-2018, 2018.

Laskin, A., Moffet, R. C., Gilles, M. K., Fast, J. D., Zaveri, R. A., Wang, B., Nigge, P., and Shutthanandan, J.: Tropospheric chemistry of internally mixed sea salt and organic particles: Surprising reactivity of NaCl with weak organic acids, J. Geophys. Res.-Atmos., 117, D15302, https://doi.org/10.1029/2012jd017743, 2012.

Li, L., Huang, Z., Dong, J., Li, M., Gao, W., Nian, H., Fu, Z., Zhang, G., Bi, X., Cheng, P., and Zhou, Z.: Real time bipolar time-of-flight mass spectrometer for analyzing single aerosol particles, Int. J. Mass Spectrom., 303, 118–124, https://doi.org/10.1016/j.ijms.2011.01.017, 2011.

Lin, Q., Zhang, G., Peng, L., Bi, X., Wang, X., Brechtel, F. J., Li, M., Chen, D., Peng, P., Sheng, G., and Zhou, Z.: In situ chemical composition measurement of individual cloud residue particles at a mountain site, southern China, Atmos. Chem. Phys., 17, 8473–8488, https://doi.org/10.5194/acp-17-8473-2017, 2017.

Ma, X., von Salzen, K., and Li, J.: Modelling sea salt aerosol and its direct and indirect effects on climate, Atmos. Chem. Phys., 8, 1311–1327, https://doi.org/10.5194/acp-8-1311-2008, 2008.

Mochida, M., Umemoto, N., Kawamura, K., and Uematsu, M.: Bimodal size distribution of C_2–C_4 dicarboxylic acids in the marine aerosols, Geophys. Res. Lett., 30, 1672, https://doi.org/10.1029/2003GL017451, 2003.

Monger, J. W., Collet Jr., J., Daube Jr., B., and Hoffmann, M. R.: Chemical composition of coastal stratus clouds: Dependence on droplet size and distance from the coast, Atmos. Environ.,

23, 2305–2320, https://doi.org/10.1016/0004-6981(89)90192-3, 1989.

Nakajima, T. Y., Suzuki, K., and Stephens, G. L.: Droplet growth in warm water clouds observed by the A-Train, Part II: A multisensor view, J. Atmos. Sci., 67, 1897–1907, https://doi.org/10.1175/2010JAS3276.1, 2010.

Nguyen, Q. T., Kjaer, K. H., Kling, K. I., Boesen, T., and Bilde, M.: Impact of fatty acid coating on the CCN activity of sea salt particles, Tellus B, 69, 1304064, https://doi.org/10.1080/16000889.2017.1304064, 2017.

Noone, K. J., Charlson, R. J., Covert, D. S., Ogren, J. A., and Heintzenberg, J.: Cloud droplets: Solute concentration is size dependent, J. Geophys. Res.-Atmos., 93, 9477–9482, https://doi.org/10.1029/JD093iD08p09477, 1988.

O'Dowd, C. D., Lowe, J. A., and Smith, M. H.: Coupling sea-salt and sulphate interactions and its impact on cloud droplets concentration predictions, Geophys. Res. Lett., 26, 1311–1314, https://doi.org/10.1029/1999gl900231, 1999.

Pekour, M. S. and Cziczo, D. J.: Wake capture, particle breakup, and other artifacts associated with counterflow virtual impaction, Aerosol Sci. Tech., 45, 758–764, https://doi.org/10.1080/02786826.2011.558942, 2011.

Petters, M. D. and Kreidenweis, S. M.: A single parameter representation of hygroscopic growth and cloud condensation nucleus activity, Atmos. Chem. Phys., 7, 1961–1971, https://doi.org/10.5194/acp-7-1961-2007, 2007.

Pierce, J. R. and Adams, P. J.: Global evaluation of CCN formation by direct emission of sea salt and growth of ultrafine sea salt, J. Geophys. Res.-Atmos., 111, D06203, https://doi.org/10.1029/2005jd006186, 2006.

Prather, K. A., Bertram, T. H., Grassian, V. H., Deane, G. B., Stokes, M. D., Demott, P. J., Aluwihare, L. I., Palenik, B. P., Azam, F., and Seinfeld, J. H.: Bringing the ocean into the laboratory to probe the chemical complexity of sea spray aerosol, P. Natl. Acad. Sci. USA, 110, 7550–7555, https://doi.org/10.1073/pnas.1300262110, 2013.

Quinn, P. K., Collins, D. B., Grassian, V. H., Prather, K. A., and Bates, T. S.: Chemistry and related properties of freshly emitted sea spray aerosol, Chem. Rev., 115, 4383–4399, https://doi.org/10.1021/cr500713g, 2015.

Roth, A., Schneider, J., Klimach, T., Mertes, S., van Pinxteren, D., Herrmann, H., and Borrmann, S.: Aerosol properties, source identification, and cloud processing in orographic clouds measured by single particle mass spectrometry on a central European mountain site during HCCT-2010, Atmos. Chem. Phys., 16, 505–524, https://doi.org/10.5194/acp-16-505-2016, 2016.

Schneider, J., Mertes, S., van Pinxteren, D., Herrmann, H., and Borrmann, S.: Uptake of nitric acid, ammonia, and organics in orographic clouds: mass spectrometric analyses of droplet residual and interstitial aerosol particles, Atmos. Chem. Phys., 17, 1571–1593, https://doi.org/10.5194/acp-17-1571-2017, 2017.

Shingler, T., Dey, S., Sorooshian, A., Brechtel, F. J., Wang, Z., Metcalf, A., Coggon, M., Mülmenstädt, J., Russell, L. M., Jonsson, H. H., and Seinfeld, J. H.: Characterisation and airborne deployment of a new counterflow virtual impactor inlet, Atmos. Meas. Tech., 5, 1259–1269, https://doi.org/10.5194/amt-5-1259-2012, 2012.

Sievering, H., Lerner, B., Slavich, J., Anderson, J., Pósfai, M., and Cainey, J.: O_3 oxidation of SO_2 in sea-salt aerosol water: Size distribution of non-sea-salt sulfate during the First Aerosol Characterization Experiment (ACE 1), J. Geophys. Res.-Atmos., 104, 21707–21717, https://doi.org/10.1029/1998jd100086, 1999.

Song, C. H. and Carmichael, G. R.: The aging process of naturally emitted aerosol (sea-salt and mineral aerosol) during long range transport, Atmos. Environ., 33, 2203–2218, https://doi.org/10.1016/S1352-2310(98)00301-X, 1999.

Sullivan, R. C. and Prather, K. A.: Investigations of the diurnal cycle and mixing state of oxalic acid in individual particles in Asian aerosol outflow, Environ. Sci. Technol., 41, 8062–8069, https://doi.org/10.1021/es071134g, 2007.

Sultana, C. M., Collins, D. B., and Prather, K. A.: Effect of structural heterogeneity in chemical composition on online single-particle mass spectrometry analysis of sea spray aerosol particles, Environ. Sci. Technol., 51, 3660–3668, https://doi.org/10.1021/acs.est.6b06399, 2017.

Tao, W. K., Chen, J. P., Li, Z. Q., Wang, C., and Zhang, C. D.: Impact of aerosols on convective clouds and precipitation, Rev. Geophys., 50, RG2001, https://doi.org/10.1029/2011rg000369, 2012.

Twohy, C. H. and Anderson, J. R.: Droplet nuclei in non-precipitating clouds: Composition and size matter, Environ. Res. Lett., 3, 045002, https://doi.org/10.1088/1748-9326/3/4/045002, 2008.

Twohy, C. H., Austin, P. H., and Charlson, R. J.: Chemical consequences of the initial diffusional growth of cloud droplets: A clean marine case, Tellus B, 41, 51–60, https://doi.org/10.1111/j.1600-0889.1989.tb00124.x, 1989.

Ueda, S., Hirose, Y., Miura, K., and Okochi, H.: Individual aerosol particles in and below clouds along a Mt. Fuji slope: Modification of sea-salt-containing particles by in-cloud processing, Atmos. Res., 137, 216–227, https://doi.org/10.1016/j.atmosres.2013.10.011, 2014.

Wang, X., Sultana, C. M., Trueblood, J., Hill, T. C., Malfatti, F., Lee, C., Laskina, O., Moore, K. A., Beall, C. M., McCluskey, C. S., Cornwell, G. C., Zhou, Y., Cox, J. L., Pendergraft, M. A., Santander, M. V., Bertram, T. H., Cappa, C. D., Azam, F., DeMott, P. J., Grassian, V. H., and Prather, K. A.: Microbial control of sea spray aerosol composition: A tale of two blooms, ACS Central Sci., 1, 124–131, https://doi.org/10.1021/acscentsci.5b00148, 2015.

Yuan, T., Li, Z., Zhang, R., and Fan, J.: Increase of cloud droplets size with aerosol optical depth: An observation and modeling study, J. Geophys. Res.-Atmos., 113, D04201, https://doi.org/10.1029/2007jd008632, 2008.

Zelenyuk, A., Imre, D., Earle, M., Easter, R., Korolev, A., Leaitch, R., Liu, P., Macdonald, A. M., Ovchinnikov, M., and Strapp, W.: In situ characterization of cloud condensation nuclei, interstitial, and background particles using the single particle mass spectrometer, SPLAT II, Anal. Chem., 82, 7943–7951, https://doi.org/10.1021/ac1013892, 2010.

Zhang, G., Bi, X., Chan, L. Y., Li, L., Wang, X., Feng, J., Sheng, G., Fu, J., Li, M., and Zhou, Z.: Enhanced trimethylamine-containing particles during fog events detected by single particle aerosol mass spectrometry in urban Guangzhou, China, Atmos. Environ., 55, 121–126, https://doi.org/10.1016/j.atmosenv.2012.03.038, 2012.

Zheng, J., Zhang, L., Che, W., Zheng, Z., and Yin, S.: A highly resolved temporal and spatial air pollutant emis-

sion inventory for the Pearl River Delta region, China and its uncertainty assessment, Atmos. Environ., 43, 5112–5122, https://doi.org/10.1016/j.atmosenv.2009.04.060, 2009.

Zheng, J. Y., Yin, S. S., Kang, D. W., Che, W. W., and Zhong, L. J.: Development and uncertainty analysis of a high-resolution NH_3 emissions inventory and its implications with precipitation over the Pearl River Delta region, China, Atmos. Chem. Phys., 12, 7041–7058, https://doi.org/10.5194/acp-12-7041-2012, 2012.